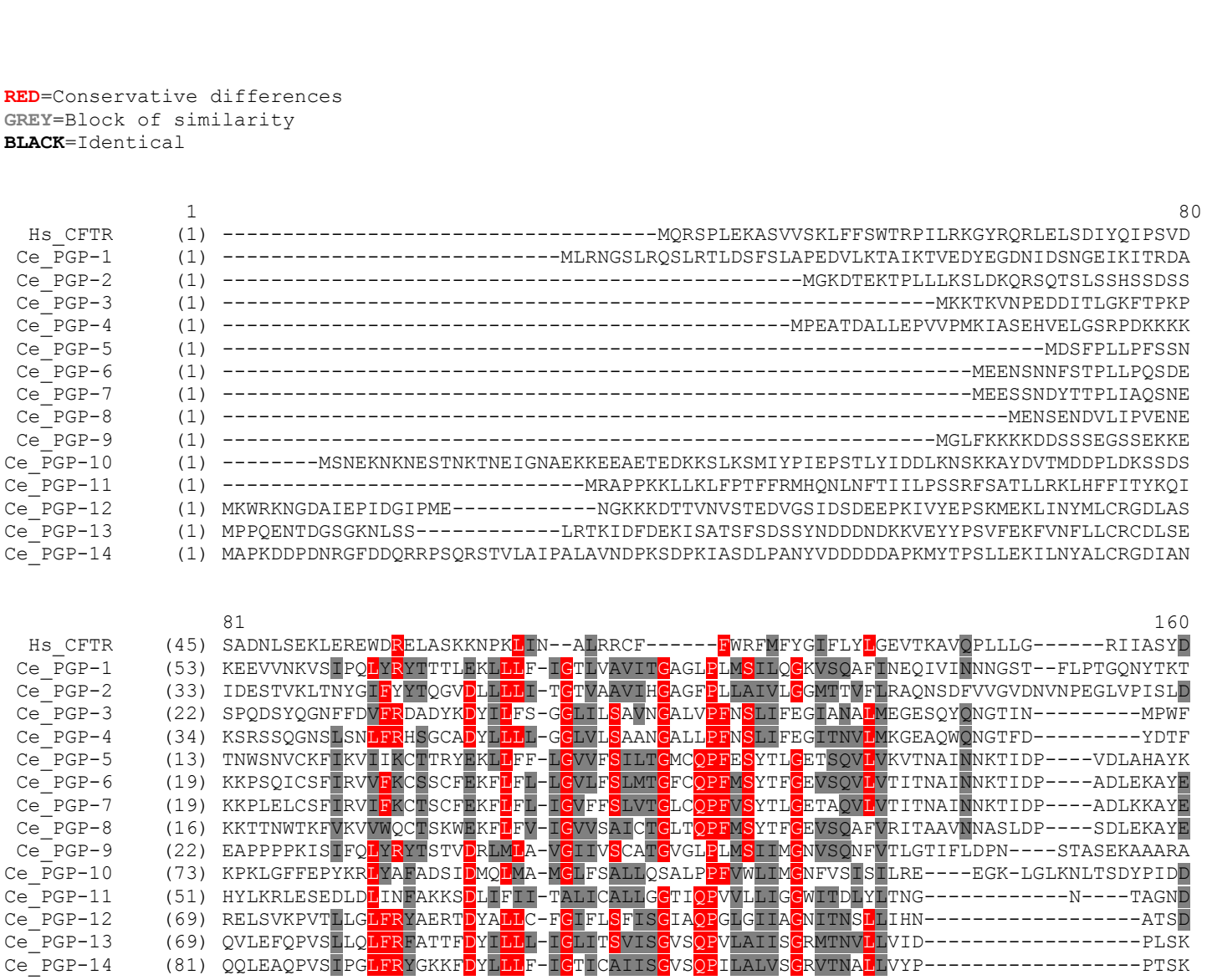

Fig. S1. Alignment of human CFTR with *C. elegans* PGP proteins. Black bar indicates the position of nucleotide binding domain 1 (NBD1). Green bar indicates the position of nucleotide binding domain 2 (NBD2). The region chimerized in the PGP-3 transgenes is boxed in yellow and the position of F508 is noted.

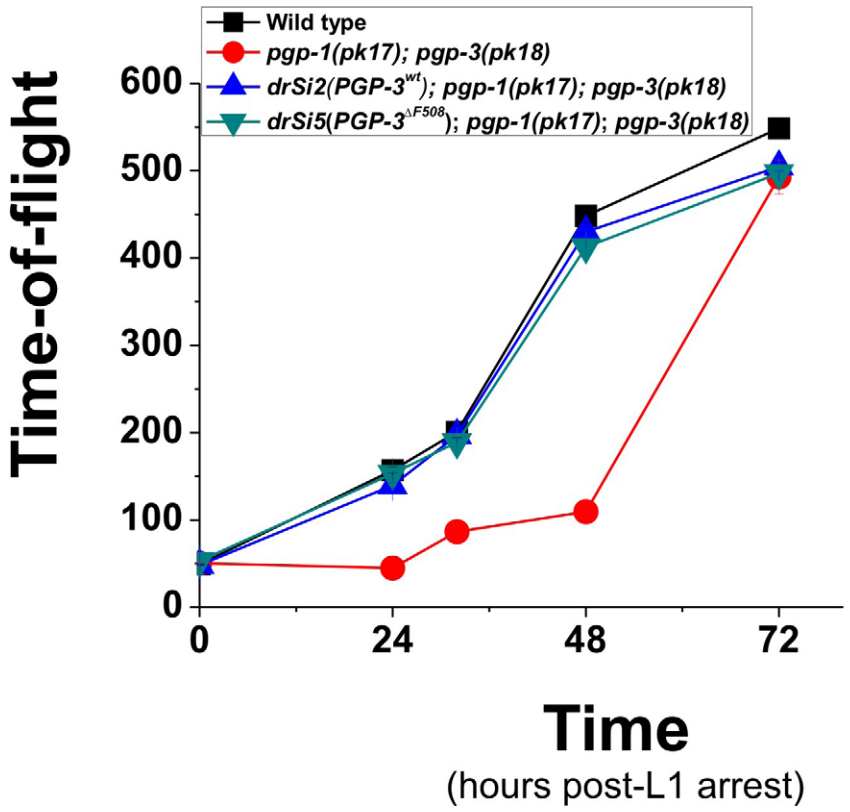

Fig. S2. Tagged *pgp-3* is functional. Single copy transgenes containing the N-terminal 3XFLAG tag and the C-terminal mCherry tag were crossed into the NL130 *pgp-1(pk17); pgp-3(pk18)* double mutant, which exhibits a reduced growth rate phenotype. The reduced growth rate is not seen in the *pgp-3(pk18)* single mutant, presumably due to functional redundancy with *pgp-1*. Hypochlorite-synchronized L1-stage animals were released from arrest by return to food plates. The size of each animal at the indicated timepoints was determined using the time-of-flight measurement on a COPAS Biosorter and analyzed as previously described (Morton and Lamitina, 2010). For each timepoint, N≥39 animals. Data shown are mean ± S.E.M.

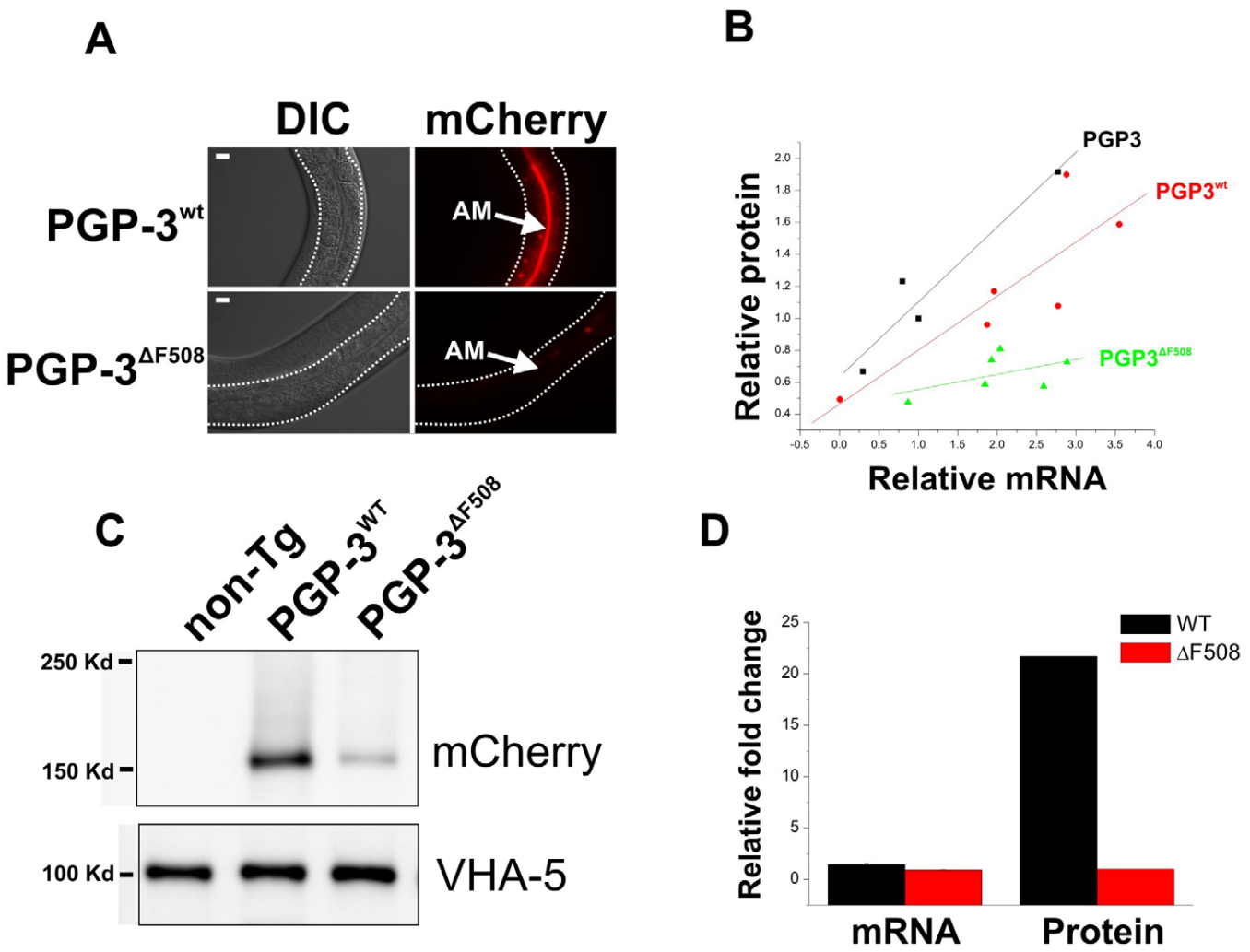

Fig. S3. PGP-3$^{\Delta F508}$ is post-transcriptionally destabilized when expressed from extrachromosomal arrays. (A) PGP-3^{wt}::mCherry and PGP-3$^{\Delta F508}$::mCherry were expressed as high-copy arrays and integrated into the genome using a UV method, as previously described (Lamitina et al., 2006). Dotted lines indicated the basolateral membrane of the intestine. The arrow points to the apical membrane of the intestine. Exposure settings in the mCherry channel are identical between the two genotypes. Scale bar=10 microns. B) Quantification of the relationship between relative mCherry fluorescent intensity and mCherry mRNA levels for non-integrated high-copy extrachromosomal arrays. 'PGP-3′ refers to transgenes expressing the unmodified *pgp-3* genomic locus fused to mCherry. The lines represent a best-fit using a linear regression fitting function. C) Western blot analysis of membrane proteins from non-transgenic wild type animals ('non-Tg'), PGP-3^{wt}, and PGP-3$^{\Delta F508}$ animals using an anti-mCherry antibody. VHA-5 is a control for equal loading. D) Quantification of mRNA (by qPCR) and protein (by fluorescence quantification) from integrated PGP-3^{wt} or PGP-3$^{\Delta F508}$ strains. Data are normalized to PGP-3$^{\Delta F508}$.

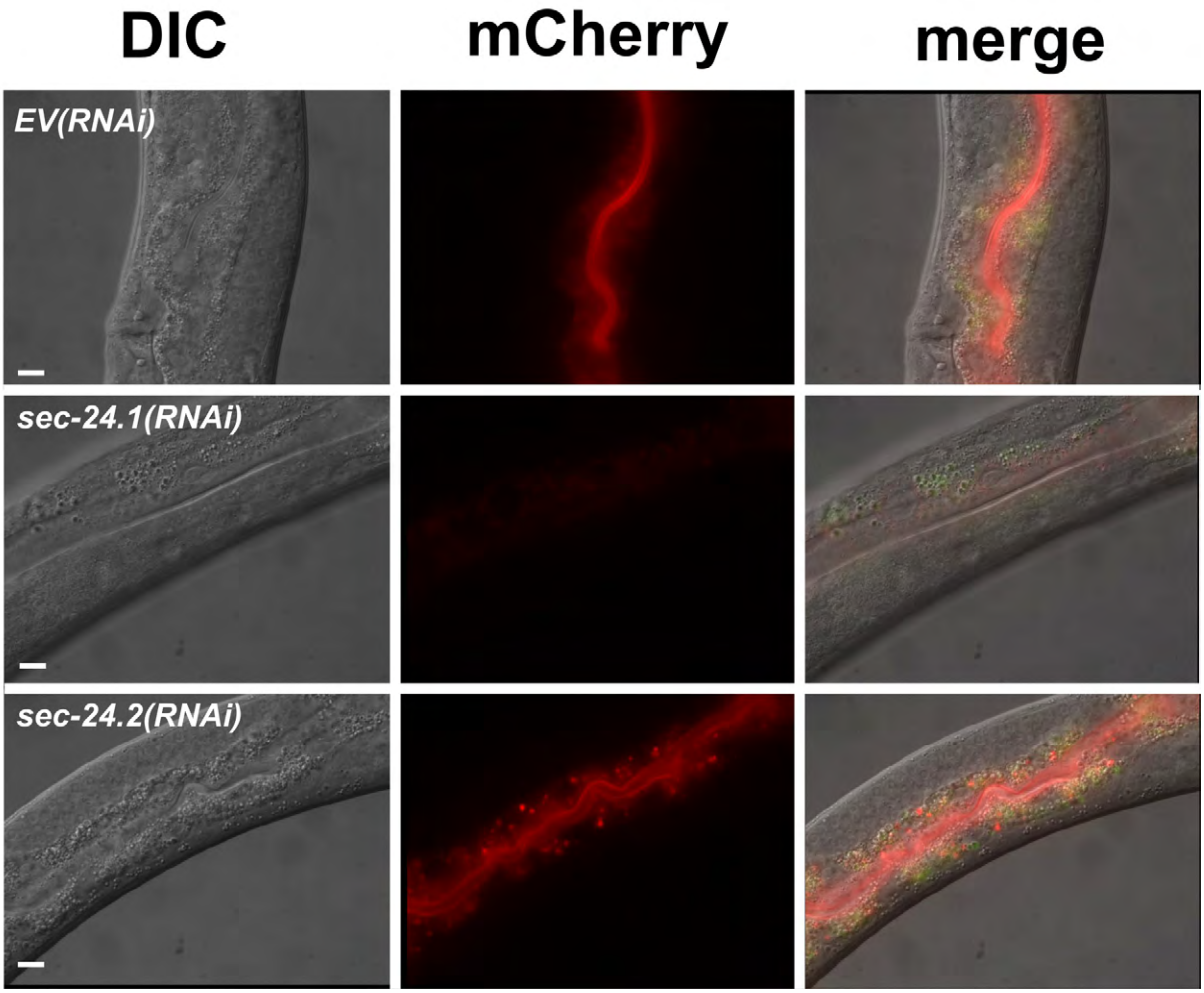

Fig. S4. PGP-3 traffics through a COPII-dependent pathway. Images of PGP-3^{wt}::mCherry expressing animals fed empty vector (EV)(RNAi), *sec-24.1(RNAi)*, or *sec-24.2(RNAi)*. Scale bar=10 microns.

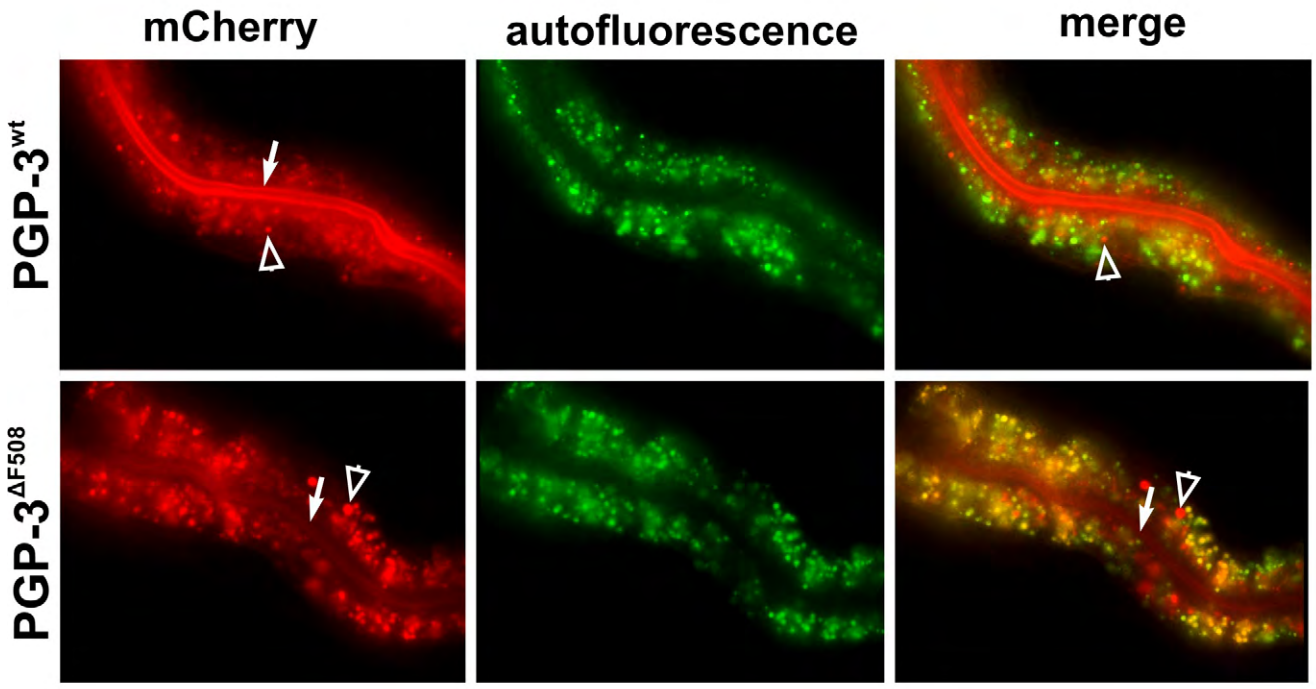

Fig. S5. Some PGP-3$^{\Delta F508}$ protein reaches the apical plasma membrane. Single-copy PGP-3^{wt}::mCherry (top) or PGP-3$^{\Delta F508}$::mCherry (bottom) animals were imaged using identical settings. Image brightness and contrast were then adjusted identically for both images to reveal PGP-3$^{\Delta F508}$::mCherry expression at the apical plasma membrane (arrow). Arrowheads indicate cytoplasmic fluorescence that does not co-localize with intestinal autofluorescence (detected using a DAPI fluorescence filter cube).

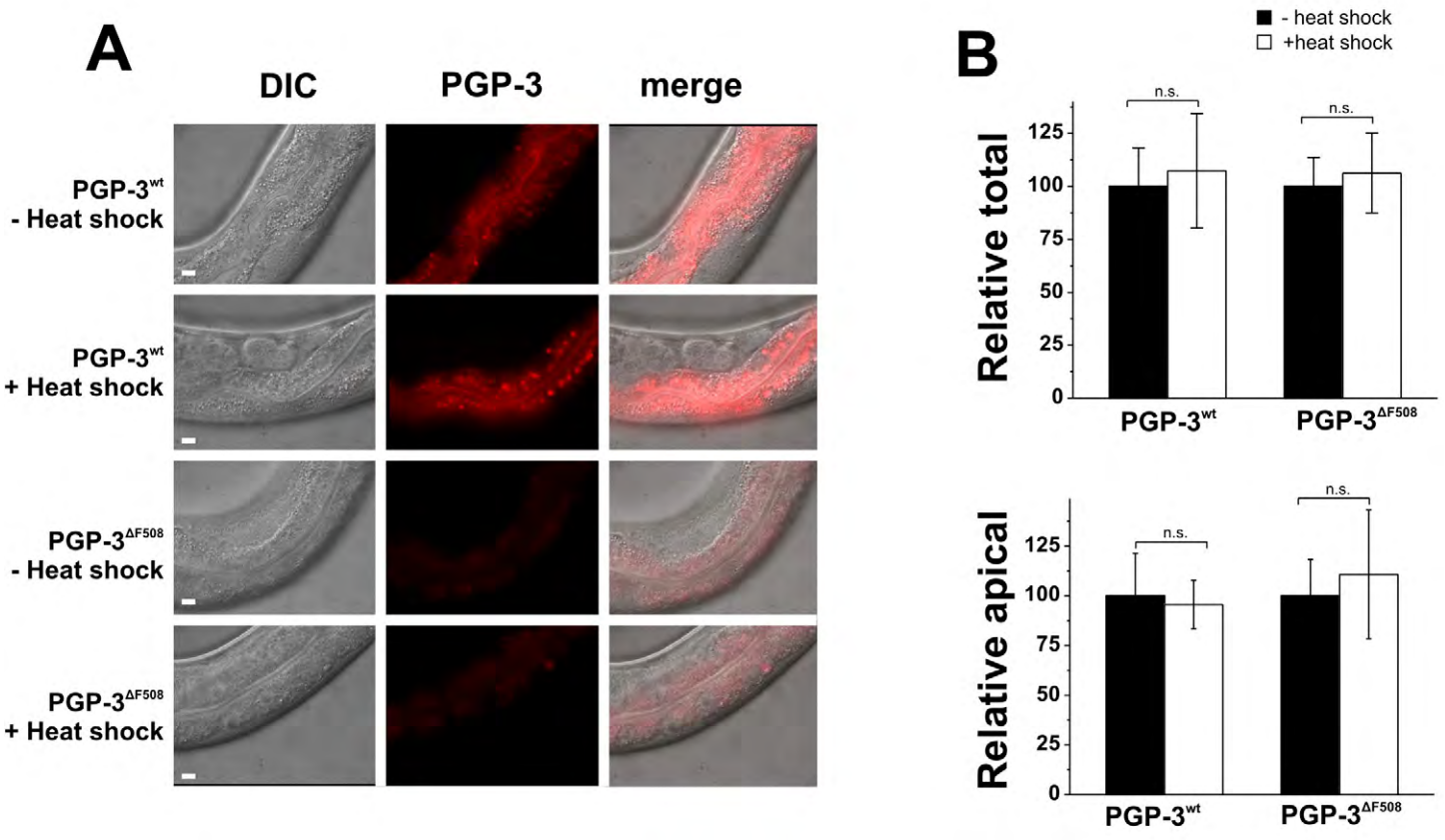

Fig. S6. Activation of the heat shock response does not stabilize PGP-3$^{\Delta F508}$. A) Images of PGP-3^{wt} or PGP-3$^{\Delta F508}$ expressing animals with and without exposure to a one hour heat shock (H.S.) at 35°C and 5 hours of recovery at 20°C. Abundance and localization of the protein was also unchanged after an additional 24 hours of recovery (not shown). Scale bar=10 microns. B) Quantification of total and apical PGP-3 abundance with and without heat shock. N=7 (PGP-3^{wt}–H.S.), 5 (PGP-3^{wt} + H.S.), 6 (PGP-3$^{\Delta F508}$)–H.S.), and 4 (PGP-3$^{\Delta F508}$ + H.S.). Data from one of two independent experiments is shown. *P*>0.5 for all.

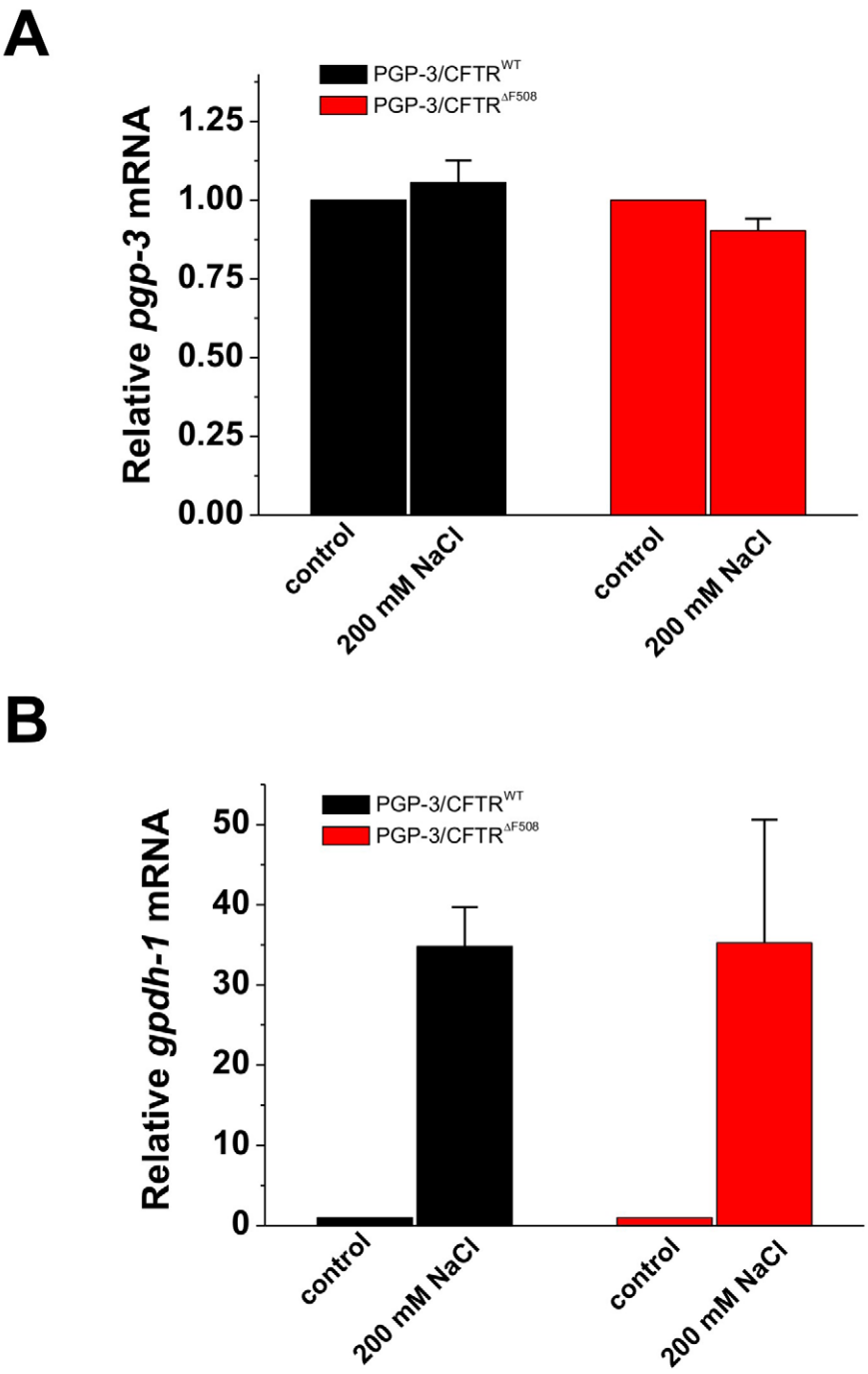

Fig. S7. Hypertonic stress does not upregulate PGP-3::mCherry expression. PGP-3^{wt} or PGP-3$^{\Delta F508}$ animals were exposed to 200 mM NaCl for 24 hours. RNA was harvested and used for quantitative PCR analysis of transgenic PGP-3 mRNA levels. Data were normalized relative to the isotonic control sample. B) Positive control showing that hypertonic stress did upregulate the expression of the organic osmolyte biosynthesis enzyme *gpdh-1*. N=4 samples per genotype.

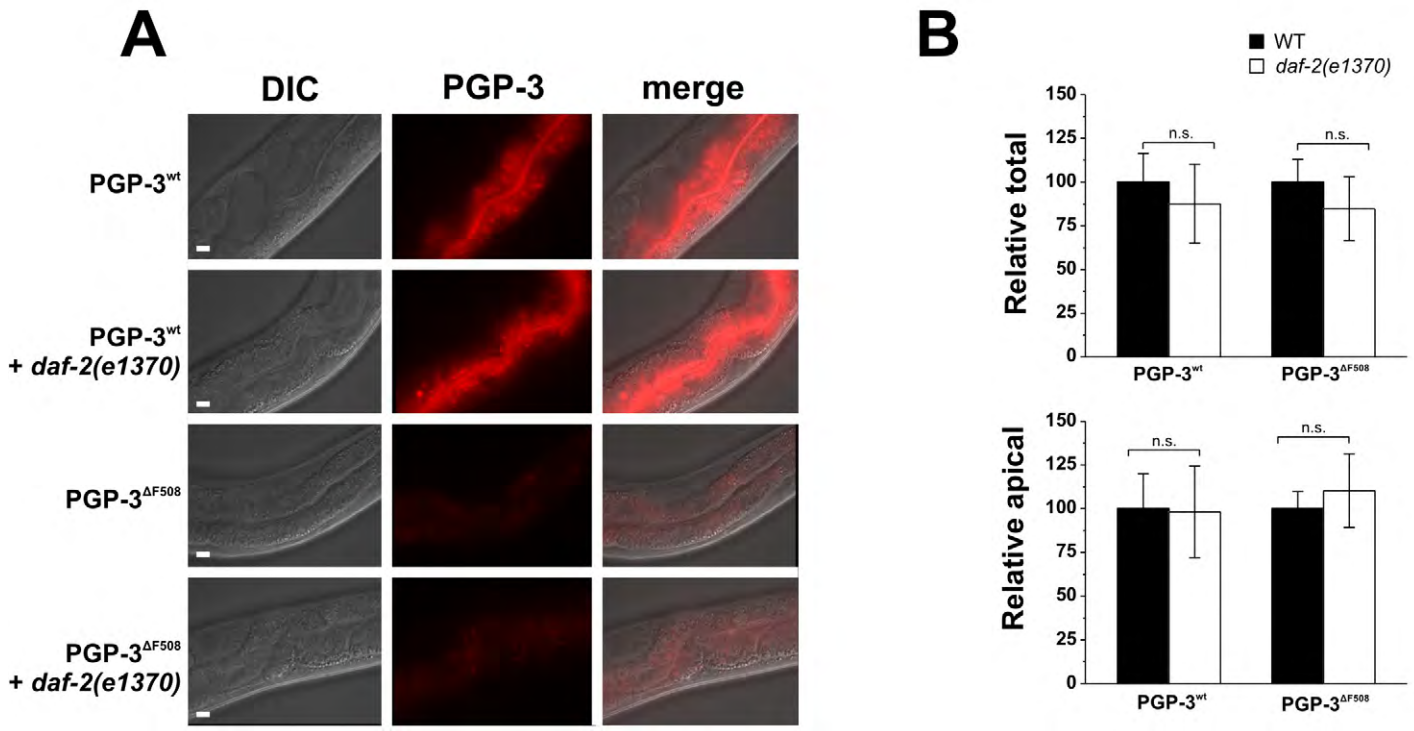

Fig. S8. Inhibition of IGF signaling does not stabilize PGP-3$^{\Delta F508}$. A) Images of PGP-3^{wt} or PGP-3$^{\Delta F508}$ expressing animals in a wild type or *daf-2(e1370)* mutant background. Scale bar=10 microns. B) Quantification of total and apical PGP-3 abundance with and without *daf-2(e1370)*. N=12 (PGP-3^{wt};+/+.), 16 (PGP-3^{wt}; *daf-2(e1370)*), 14 (PGP-3$^{\Delta F508}$; +/+), and 11 (PGP-3$^{\Delta F508}$; *daf-2(e1370)*). Data from one of two independent experiments is shown. P>0.5 for all.

Table S1. Percent Identity among *C. elegans* PGPs and human CFTR

	Hs_CFTR	Ce_PGP-1	Ce_PGP-2	Ce_PGP-3	Ce_PGP-4	Ce_PGP-5	Ce_PGP-6	Ce_PGP-7	Ce_PGP-8	Ce_PGP-9	Ce_PGP-10	Ce_PGP-11	Ce_PGP-12	Ce_PGP-13	Ce_PGP-14
Hs_CFTR	100	13	15	**15**	16	16	16	15	15	14	14	16	14	14	14
Ce_PGP-1		100	42	**38**	38	37	38	38	37	52	28	29	37	36	38
Ce_PGP-2			100	**39**	38	35	36	35	36	43	30	34	37	37	37
Ce_PGP-3				**100**	**77**	**34**	**35**	**35**	**33**	**42**	**29**	**33**	**38**	**37**	**39**
Ce_PGP-4					100	35	37	37	35	41	29	33	39	37	39
Ce_PGP-5						100	68	68	58	38	29	29	33	32	33
Ce_PGP-6							100	96	63	39	28	29	34	34	34
Ce_PGP-7								100	62	39	29	29	34	33	34
Ce_PGP-8									100	38	29	29	32	32	33
Ce_PGP-9										100	28	32	36	38	39
Ce_PGP-10											100	28	27	27	27
Ce_PGP-11												100	34	34	35
Ce_PGP-12													100	62	65
Ce_PGP-13														100	72
Ce_PGP-14															100

Table S2. Effect of ERAD gene knock-down on PGP-3$^{\Delta F508}$ and PGP-3^{wt} intestinal fluorescence.

		Relative intestinal fluorescence[1] [mean intensity%±standard deviation (n)^{significance}]													
		PGP-3$^{\Delta F508}$										**PGP-3^{wt}**			
		Total mCherry (trials)					**Apical mCherry (trials)**					**Total**		**Apical**	
C. elegans	mammalian homologue	1	2	3	4	5	1	2	3	4	5	1	2	1	2
cdc-48.1 (MRC)	p97	224±16 (4)**	248±34 (7)**				222±18 (4)**	206±39 (4)**							
cdc-48.2 (MRC)	p97	212§±94 (8)**	324§±68 (13)**	347§±57 (12)**	241±36 (9)**	298±42 (7)**	224§±107 (8)**	275§±59 (12)**	274§±42 (10)**	187±27 (6)**	237±26 (5)**	101±19 (11)^{ns}		102±22 (10)^{ns}	
cdc-48.2 (ORF)	p97	159§±33 (7)**	218§±28 (9)**	170§±27 (7)**	93±20 (10)^{ns}	120±17 (5)^{ns}	122§±30 (7)^{ns}	189§±36 (8)**	109§±18 (7)^{ns}	70±17 (8)^{ns}	87±20 (4)^{ns}				
cdc-48.3 (MRC)	p97	117§±26 (8)^{ns}	119±17 (5)^{ns}				106§±25 (8)^{ns}	111±17 (5)^{ns}				96±18 (9)^{ns}		93±19 (8)^{ns}	
cnx-1 (mutant)	calnexin	99±10 (10)^{ns}	109±12 (9)^{ns}				103±14 (10)^{ns}	98±13 (9)^{ns}							
crt-1 (MRC)	calreticulin	151§±10 (7)*	154§±22 (8)**	120§±20 (6)^{ns}	128±10 (7)**		170§±13 (7)**	142§±9 (8)*	110§±19 (6)^{ns}	111±14 (7)^{ns}		95±12 (12)^{ns}	112±19 (10)^{ns}	93±17 (12)^{ns}	119±27 (10)^{ns}
cup-2 (MRC)	Derlin-1	116§±25 (8)^{ns}	97§±19 (5)^{ns}				128§±30 (8)^{ns}	86§±19 (5)^{ns}							
cup-2 (mutant)	Derlin-1	113± 13 (11)^{ns}	129±11 (6)**				108±17 (11)^{ns}	142±13 (6)**							
hsp-3 (MRC)	GRP78/BiP	129§±27 (7)^{ns}	114§±14 (12)^{ns}	97±9 (6)^{ns}			137§±29 (7)^{ns}	105§±15 (12)^{ns}	79±6 (6)^{ns}						
hsp-3 (mutant)	GRP78/BiP	113±16 (10)^{ns}	89±22 (11)^{ns}				123±16 (10)**	91±21 (11)^{ns}							
marc-6 (MRC)	TEB4	129§±15 (10)^{ns}	128§±30 (12)^{ns}	102§±17 (9)^{ns}	92±14 (5)^{ns}		154§±28 (10)*	122§±27 (12)^{ns}	102§±21 (9)^{ns}	76±15 (5)^{ns}					
R151.6 (MRC)	Derlin-2	171§±45 (10)**	158§±37 (10)**	143§±30 (9)*	152±14 (9)**	125±34 (7)^{ns}	193§±47 (10)**	160§±39 (10)**	134§±31 (9)*	156±10 (9)**	124±34 (7)^{ns}	121±16 (13)*	114±26 (11)^{ns}	105±19 (13)^{ns}	122±33 (11)^{ns}
rnf-5 (mutant)	RMA1/GRP78/ RNF5	128±11 (9)**	132±11 (9)**				141±14 (9)**	143±20 (9)**							
rpt-6 (ORF)		113§±17 (10)^{ns}	107§±23 (6)^{ns}	95±16 (6)^{ns}			119§±11 (10)^{ns}	103§±30 (6)^{ns}	85±18 (6)^{ns}						
wwp-1 (MRC)	Nedd4-2	92±20 (15)^{ns}	96§±15 (9)^{ns}	111±14 (9)^{ns}	117±10 (6)^{ns}		114±30 (15)^{ns}	96§±20 (9)^{ns}	121±17 (9)*	129±13 (6)*					

[1] – all data are normalized to control measurements (either PGP-3$^{\Delta F508}$ in a wild type background (for mutant analysis) or PGP-3^{wt} and PGP-3$^{\Delta F508}$ fed empty vector dsRNA (for RNAi experiments). Control data were obtained in parallel to the experimental data using identical imaging conditions.

§= measured at the L4 stage

*=p<0.05, **=p<0.01, ns= not significant